frontiers in Physics

ORIGINAL RESEARCH
published: 28 April 2021
doi: 10.3389/fphy.2021.642754

A Thermodynamic Framework for Stretching Processes in Fiber Materials

A. Arango-Restrepo[1,2], *J. M. Rubi*[1,2,3] *and Srutarshi Pradhan*[3]*

[1]*Departament de Fisica de La Matèria Condensada, Universitat de Barcelona, Barcelona, Spain,* [2]*Institut De Nanociencia I Nanotecnologia, Universitat De Barcelona, Barcelona, Spain,* [3]*PoreLab, Department of Physics, Norwegian University of Science and Technology, Trondheim, Norway*

Fiber breakage process involves heat exchange with the medium and energy dissipation in the form of heat, sound, and light, among others. A purely mechanical treatment is therefore in general not enough to provide a complete description of the process. We have proposed a thermodynamic framework which allows us to identify new alarming signals before the breaking of the whole set of fibers. The occurrence of a maximum of the reversible heat, a minimum of the derivative of the dissipated energy, or a minimum in the stretching velocity as a function of the stretch can prevent us from an imminent breakage of the fibers which depends on the nature of the fiber material and on the load applied. The proposed conceptual framework can be used to analyze how dissipation and thermal fluctuations affect the stretching process of fibers in systems as diverse as single-molecules, textile and muscular fibers, and composite materials.

Keywords: fiber bundle model, alarming signal, mesoscopic nonequilibrium thermodynamics, Fokker–Planck equation, dissipation, entropy production

OPEN ACCESS

Edited by:
Antonio F. Miguel,
University of Evora, Portugal

Reviewed by:
Antonio Heitor Reis,
University of Evora, Portugal
Zhi Zeng,
Hefei Institutes of Physical Science (CAS), China

***Correspondence:**
Srutarshi Pradhan
srutarshi.pradhan@ntnu.no

Specialty section:
This article was submitted to Interdisciplinary Physics, a section of the journal Frontiers in Physics

Received: *16 December 2020*
Accepted: *08 February 2021*
Published: *28 April 2021*

Citation:
Arango-Restrepo A, Rubi J M and Pradhan S (2021) A Thermodynamic Framework for Stretching Processes in Fiber Materials. Front. Phys. 9:642754. doi: 10.3389/fphy.2021.642754

1 INTRODUCTION

When external load/stretch is applied on fiber materials composed of elements with different strength thresholds, weaker elements fail first. As the surviving elements have to support the load, stress (load per element) increases and that can trigger more element failure. With continuous loading/stretching, at some point the system collapses completely, that is, the external load/stretch is above the strength of the whole system at that point. Such a system collapse is known as "catastrophic failure" for that system.

There are several physics-based approaches [1–3] that can model such a scenario. Fiber bundle model (FBM) is one of those models, and FBM has become a useful tool for studying fracture and failure [4–6] of composite materials under different loading conditions. The simplicity of the model allows achieving analytic solutions [5, 7] to an extent that is not possible in any of the fracture models studied so far. For these reasons, FBM is widely used as a model of breakdown that extends beyond disordered solids. In fact, fiber bundle model was first introduced by a textile engineer [4]. Later, physicists took interest in it, mainly to explore the failure dynamics and avalanche phenomena in this model [8–10]. Furthermore, it has been used as a model for other geophysical phenomena, such as snow avalanche [11], landslides [12, 13], biological materials [14], or even earthquakes [15].

Although stretching processes in FBM have been analyzed extensively [1–6], mainly by the physics community, a concrete thermodynamic description for the stretching process is still lacking in this field. In the efforts to unveil the stretching failure phenomena, thermodynamics

seems to be an important tool because it allows incorporating variables such as temperature, entropy, reversible heat, entropy production rate, and energy dissipation to thus unify stretching failure dynamics and energy analysis, especially where surface effects, heat release, and sound emission, due to energy dissipation, are present when dealing with the stretching failure of fibrous materials.

In this article, we intend to develop a thermodynamic framework to analyze not only the energetics of the stretching failure phenomena but also the dynamics by means of nonequilibrium thermodynamic formalism at all scales, from a single molecule to a macrostructure. We believe that our thermodynamic framework could carry over to other problem areas, eventually also outside the physical sciences such as molecular biology and nanotechnology.

We arrange the article as follows: After the Introduction (**section 1**), we give a short background of studies on stretching of FBM in **section 2**. In several subsections of **section 2**, we discuss strength and stability in FBM, energy variations during stretching, and warning signs of catastrophic failure. In **section 3**, we introduce a proper thermodynamic framework of the stretching process and analyze the mesoscopic regime and small-fluctuation regime. All the simulation results are presented in **section 4**, including dynamics and energetics, the Fokker–Plank approach, and the role of fluctuations on the stretching process. We make some conclusions at the end (**section 5**).

2 BACKGROUND: STRETCHING OF A FIBER BUNDLE

In 1926, F. T. Peirce introduced the fiber bundle model [4] to study the strength of cotton yarns in connection with textile engineering. Some static behavior of such a bundle (with equal load sharing by all the surviving fibers, following a failure) was discussed by Daniels in 1945 [16], and the model was brought to the attention of physicists in 1989 by Sornette [17].

In this model, a large number of parallel Hookean springs or fibers are clamped between two horizontal platforms; the upper one (rigid) helps hanging the bundle, while the load hangs from the lower one. The springs or fibers are assumed to have different breaking strengths. Once the load per fiber exceeds a fiber's own threshold, it fails and cannot carry the load any more. The load/stress it carried is now transferred to the surviving fibers. If the lower platform deforms under loading, fibers closer to the just-failed fiber will absorb more of the load than those further away, and this is called the local load sharing (LLS) scheme [18]. On the other hand, if the lower platform is rigid, the load is equally distributed to all the surviving fibers. This is called the equal load sharing (ELS) scheme. Intermediate range load redistribution is also studied (see [19]).

2.1 Strength and Stability in a Fiber Bundle Model

Let us consider a fiber bundle model having N parallel fibers placed between two stiff bars (**Figure 1**). Under an external force,

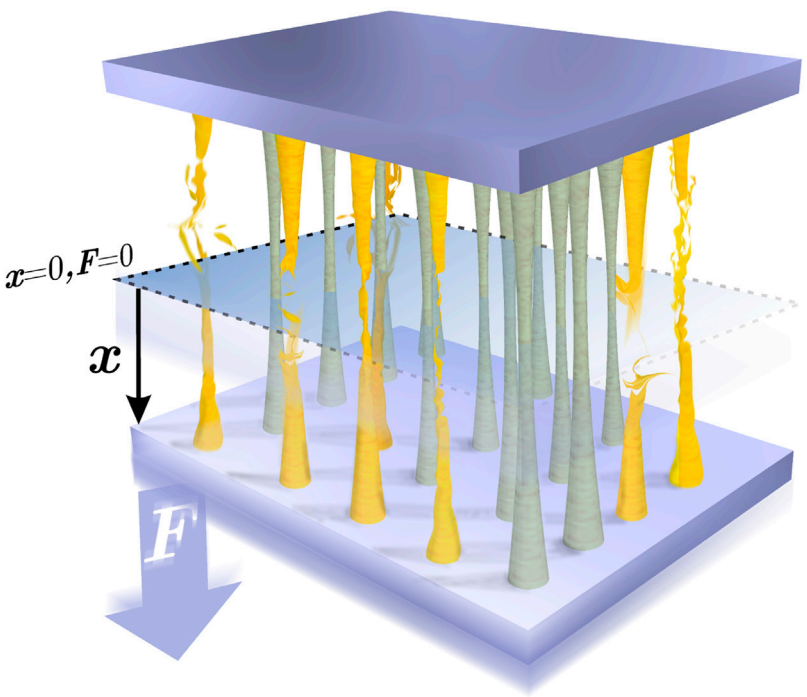

FIGURE 1 | Illustration of the system. Under the application of a constant external force F, the set of fibres are stretched by a length x. As the fibers have different strength thresholds, some of them break (yellow fibres) resulting in the increment of load for the non-broken fibres (grey fibres).

the system responds linearly with an elastic force. The dimensionless elastic force F_e for a given dimensionless stretch value x (ranging from 0 to 1) is $F_e = \kappa x$, where κ is the dimensionless spring constant $\kappa = k_e L_m/F$ with k_e as the elastic constant of the material, L_m as the maximum stretching length, and F as the external force (applied load). If the stretch x exceeds this threshold, the fiber fails irreversibly. In the equal load sharing (ELS) model, the bars are stiff and the applied load F is shared equally by the intact fibers.

2.1.1 Fiber Strength Distribution

The strength thresholds of the fibers are drawn from a probability density $p(x)$. The corresponding cumulative probability is given by

$$P(x) = \int_0^x p(y)dy \tag{1}$$

from which we can obtain the number of non-broken fibers as a function of the average deformation of the set of fibers x:

$$n(x) = N[1 - P(x)]. \tag{2}$$

The fraction of broken fibers, or damage, is then given by $m(x) = 1 - n(x)/N$. For a uniform distribution, one has $p(x) = 1$, $P(x) = x$, and $n(x) = N(1 - x)$.

2.1.2 The Critical/Failure Strength

The bundle exhibits an elastic force

$$F_e(x) = N[1 - P(x)]\kappa x. \tag{3}$$

The normalized elastic force (F_e/N) vs. the average stretch x is represented in **Figure 2** for a uniform probability distribution.

The elastic force maximum is the strength of the bundle and the corresponding stretch value (x_c) is the critical stretch beyond which the bundle collapses. Two distinct regimes of the system can be recognized: one stable, for $0 < x \leq x_c$, and another unstable, for $x > x_c$.

The critical stretch value follows from the condition $dF_e/dx = 0$. In the case of a uniform threshold distribution, using the corresponding values of $p(x_c)$ and $P(x_c)$, we obtain $x_c = 1/2$.

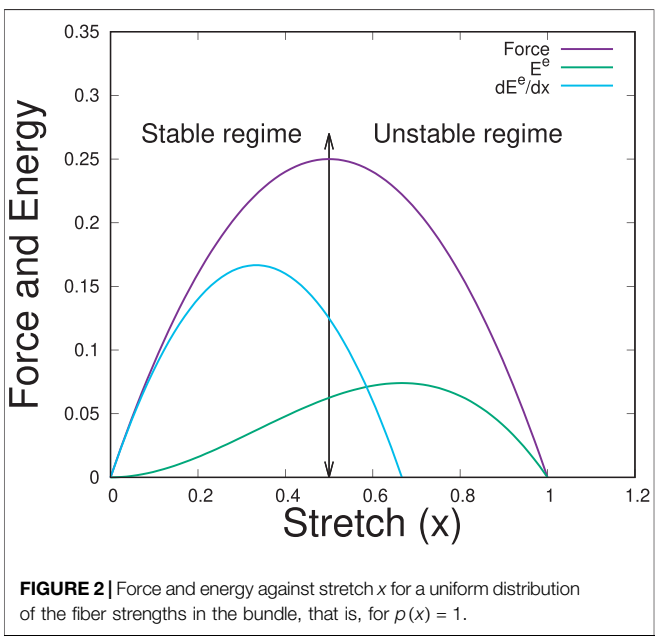

FIGURE 2 | Force and energy against stretch x for a uniform distribution of the fiber strengths in the bundle, that is, for $p(x) = 1$.

2.2 Energies in Fiber Bundle Model During Stretching

When N is large, one can express the elastic E_e and the breaking E_b energies in terms of the stretch x as

$$E_e(x) = \frac{N\kappa}{2} x^2[1 - P(x)] \tag{4}$$

and

$$E_b(x) = \frac{N\kappa}{2} \int_0^x dy[p(y)y^2]. \tag{5}$$

For a uniform distribution within the range $(0, 1)$, setting $p(x) = 1$ and $P(x) = x$ in **Eqs. 4**, **5**, we get $E_e(x) = \frac{N\kappa}{2} x^2(1 - x)$ and $E_b(x) = \frac{N\kappa}{6} x^3$. Clearly, breaking energy increases steadily with the stretch, but elastic energy reaches a maximum (see **Figure 2**).

2.3 The Warning Signal of a Catastrophic Failure

The elastic energy reaches a maximum value which falls in the unstable region of **Figure 2**, after the critical value of the extension. Its knowledge is thus not useful to predict the catastrophic failure point of the system. However, the maximum value x_{max} of dE_e/dx appears before x_c (see **Figure 2**). To obtain the relation between x_{max} and x_c, we take the derivative of dE_e/dx, with respect to x, in which for a uniform distribution, the solution of $d^2E_e(x)/dx^2 = 0$ gives

$$x_{max} = \frac{2}{3} x_c. \tag{6}$$

The rate of change of the elastic energy thus shows a peak before the failure comes [20].

3 THERMODYNAMICS OF STRETCHING PROCESSES

The stretching failure of fibers/materials is seen at a small scale, for example, during stretching of molecules in biological objects [21]. Similar stretching failure phenomena are also observed on a much bigger scale, like in the case of bridges made of long cables [22]. The observation in Ref. [20] that elastic energy variation could be a useful indicator of upcoming stretching-induced failure motivates us to construct a proper thermodynamic framework for such stretching failure phenomenon. For this purpose, we are going to introduce some new concepts like thermal bath, irreversible energy dissipation, and entropy production, and we believe that such a framework will help explore some new features of stretching failure behavior in

general. In this section, we will compute the energy dissipated and the heat released in the stretching process and show that dissipation provides a warning signal of the failure.

3.1 Energetics

Due to the load F, the system experiences an external work W which affects the elastic and breaking energies and the entropy S as well. Energy conservation can thus be formulated as

$$W = \Delta E_e + \Delta E_b + T\Delta S, \tag{7}$$

where $T\Delta S$ is the heat released Q_r in the process and ΔE_d the energy dissipated, with T the temperature. All the terms in this equations are measured in units of FL_mN. The elastic energy of the fibers as a function of the elongation results from the elastic energy per fiber times the number of unbroken fibers (**Eq. 2**):

$$\Delta E_e(x) = \frac{n(x)}{N}\varphi(x), \tag{8}$$

where $\varphi(x) = \frac{\kappa}{2}x^2$. The breaking energy results from the elastic energy which transforms into kinetic and surface energy. An infinitesimal change of this energy is related to the infinitesimal change of the damage through $dE_b(x) = \varphi(x)dm(x)$. Therefore, its total change is

$$\Delta E_b(x) = \int_0^x \varphi(z)\left[\frac{\partial m(z)}{\partial z}\right]dz. \tag{9}$$

The work done by the external force is the sum of the work done on each fiber:

$$W(x) = \frac{1}{FN}\sum_{i=1}^{n(x)} w_i(x) \approx \frac{1}{FN}\int_0^n w(x)dn', \tag{10}$$

where the work per fiber w is

$$w_i(x) = -\int_0^x \frac{F}{n(y)}dy. \tag{11}$$

Changes in the entropy in the stretching process are expressed as

$$\Delta S = \Delta_r S + \Delta_i S, \tag{12}$$

where $\Delta_r S$ is the entropy supplied to the system by its surroundings and $\Delta_i S$ is the entropy produced in the process. The second law of thermodynamics states that $\Delta_i S \geq 0$, where the zero value holds for reversible stretching (at quasi-equilibrium). The entropy supplied can be positive or negative; the sign depends on the interaction of the system with its surroundings [23]. For a closed system that may exchange heat with the surroundings, it is given by the Carnot–Clausius expression

$$\Delta_r S = \frac{Q_r}{T}, \tag{13}$$

where Q_r is the reversible or compensated heat, supplied for the surroundings, and T is the temperature of the environment. The irreversible change of the entropy, or the total entropy produced, at average elongation x is given by

$$\Delta_i S = \int_0^t \frac{n(x)}{N}\sigma dt', \tag{14}$$

where σ is the entropy production rate. The Goudy–Stodola theorem relates the total energy dissipated ΔE_d to the entropy produced $\Delta_i S$ [24]:

$$\Delta E_d = T\Delta_i S. \tag{15}$$

At this point, it is important to distinguish between reversible heat Q_r and dissipated energy E_d. The former is the energy in the form of heat supplied from or toward the surroundings in order to keep the temperature of the system constant. This quantity can be measured, for instance, by using a calorimeter. The latter is the free energy lost that can be transferred as heat, sound, or light, to mention just few forms of energy. The energy dissipated is thus not necessarily related to a measurable heat flux or to a measurable temperature change in the neighborhood of the system. This is the reason why reversible heat is frequently referred on the literature as measurable heat [23].

3.2 Mesoscopic Nonequilibrium Thermodynamics

When the fibers are immersed in a heat bath, their length can fluctuate. The effect of these fluctuations is negligible when the energy of the fibers is much greater than the thermal energy k_BT, which is the limit of validity of a purely mechanical treatment. For smaller system energies, the fluctuations become increasingly important. This is the case, for example, in the stretching of DNA [25]. Here, we analyze the dynamics of the elongation fluctuations and compute the entropy production rate and the energy dissipated in the process.

The probability density $\rho(x,t)$ to find a fiber with length x at dimensionless time t fulfills the continuity equation

$$\frac{\partial \rho(x,\,t)}{\partial t} = -\frac{\partial J(x,\,t)}{\partial x} \tag{16}$$

ensuing from probability conservation. In this equation, J is the probability current which vanishes at the boundaries ($x = 0$ and $x = 1$). The entropy production rate σ of the stretching process follows from mesoscopic nonequilibrium thermodynamics [26]:

$$\sigma(t) = -\frac{1}{T}\int_0^1 J(x,t)\frac{\partial \mu(x,t)}{\partial x}dx. \tag{17}$$

By coupling linearly, the flux J and its conjugated thermodynamic force (chemical potential gradient $\partial\mu/\partial x$), we obtain the dimensionless current

$$J(x,t) = -\rho(x,t)\frac{\partial \mu(x,t)}{\partial x} \tag{18}$$

which corresponds to Fick's diffusion law written in a dimensionless form where $t = t'D/L_m^2$ is the dimensionless time and D is the diffusivity [26]. The chemical potential is related to the free energy of the system through $\mu(x,t) = \left(\frac{\partial G}{\partial n}\right)_{T,P}$, which in turn is given by

$$\begin{aligned}\Delta G &= \Delta H - T\Delta_r S \\ &= \int_0^n \int_0^x \frac{1}{n(y)}dydn - n(x)\frac{\varphi(x)}{N} + \frac{k_BT}{FL_m}n(x)\ln\rho(x)\end{aligned} \tag{19}$$

with H being the enthalpy to which the elongation work and the elastic (potential) energy contribute. From now on, we will use the dimensionless force per fiber $f = FL_m/k_BT$. Taking the derivative of the Gibbs free energy with respect to the number of non-broken fibers n and considering **Eq. 2**, we obtain the chemical potential

$$\mu(x,t) = \int_0^x \frac{1}{n(y)}dy - \varphi(x) + \frac{1}{f}\ln\rho. \tag{20}$$

For large values of f, the entropic contribution is very small. Notice that the signs of the enthalpic terms have been changed because the external work is done in the direction of the movement, while the elastic force has the opposite direction.

Substituting **Eq. 20** in **Eq. 18** and the resulting flux in **Eq. 16**, we obtain the Fokker–Planck equation describing the evolution of the probability distribution

$$\frac{\partial\rho(x,t)}{\partial t} = \frac{\partial}{\partial x}\left[N\frac{\rho(x,t)}{n(x)} - \rho(x,t)\frac{\partial\varphi(x)}{\partial x} + \frac{1}{f}\frac{\partial\rho(x,t)}{\partial x}\right]. \tag{21}$$

The average elongation of the fibers corresponds to the first moment of the probability density ρ, and the solution of this equation is

$$\overline{x}(t) = \int_0^1 x\rho(x,t)dx. \tag{22}$$

Taking the time derivative of **Eq. 22** and using the conservation law (**Eq. 16**), we obtain

$$\dot{\overline{x}}(t) = \int_0^1 J(x,t)dx \tag{23}$$

from which we can interpret J as the local stretching velocity.

3.3 Small Fluctuation Regime

When fluctuations are very small, the variance of the probability distribution takes very small values, and therefore, we could approximate $\rho(x,t)$ by a delta function centered on $\overline{x}$: $\delta[x-\overline{x}(t)]$. By combining **Eqs. 18**, **20** and substituting $\rho(x,t)$ by the delta function, we obtain

$$J(x,t) = \delta[x-\overline{x}(t)]\left(\frac{1}{f} + \frac{N}{n(x)} - \kappa x\right), \tag{24}$$

where we have used the definition of φ. Integrating now **Eq. 24** in x, we obtain the stretching velocity

$$\dot{\overline{x}}(t) = \frac{1}{f} + \frac{N}{n(\overline{x})} - \kappa\overline{x}, \tag{25}$$

where the first term on the right side is the entropic contribution, the second results from the presence of the load, and the third is due to the elastic force which opposes to the elongation of the fibers. For very small fluctuations, the entropy production rate **Eq. 17** is $\sigma(t) = \dot{\overline{x}}^2$. Using this result into **Eq. 14**, and the equality $\dot{\overline{x}} = d\overline{x}/dt$, we obtain the irreversible entropy change

$$\Delta_i S(\overline{x}) = \int_0^{\overline{x}} \frac{n(\overline{x})}{N}\dot{\overline{x}}d\overline{x}. \tag{26}$$

4 RESULTS AND DISCUSSION

In this section, we obtain analytic expressions and numerical results for the dynamics and energetics of the stretching process assuming a uniform distribution of the strength thresholds of the fibers, $P(x) = x$. In order to simplify the notation, from now on, x will stand for the average value $\overline{x}$.

4.1 Dynamics and Energetics for Small Fluctuations

4.1.1 Dynamics

The average stretching velocity for a uniform distribution is obtained from **Eq. 25**, which is now written as

$$\dot{x}(t) = \frac{1}{f} + \frac{1}{1-x} - \kappa x. \tag{27}$$

Its derivative with respect to the elongation given by

$$\frac{d\dot{x}(t)}{dx} = \frac{1}{(1-x)^2} - \kappa \tag{28}$$

has a minimum around $x = 1 - \sqrt{1/\kappa}$, for $\kappa \geq 1$, indicating that for large enough values of κ, the stretching velocity exhibits a non-monotonic behavior. By integrating **Eq. 27**, we obtain the expression relating t and x:

$$t = -\frac{1}{2\kappa}\ln[1-\kappa x(1-x)] - \frac{1}{\sqrt{(4-\kappa)\kappa}}\left\{\tan^{-1}\left[\frac{\sqrt{\kappa}(1-2x)}{\sqrt{4-\kappa}}\right] - \tan^{-1}\left(\frac{\sqrt{\kappa}}{\sqrt{4-\kappa}}\right)\right\}. \tag{29}$$

For $\kappa \geq 4$, this equation diverges or is imaginary, which indicates that the process is not possible. From this relation, we can anticipate the asymptotic form of x through the behavior of the inverse tangent.

4.1.2 Energetics

From the dynamic of the process, we can compute the work, the energies, and the heat involved. The work follows from **Eqs. 10**, **11**:

$$W = -x(\ln x - 1). \tag{30}$$

The breaking energy, computed from **Eq. 9**, is

$$\Delta E_b = \frac{\kappa}{6}x^3. \tag{31}$$

As expected, the breaking energy increases as the elongation increases. From **Eq. 8**, the elastic energy change is

$$\Delta E_e = \frac{\kappa}{2}(1-x)x^2, \tag{32}$$

and its derivative

$$\frac{d\Delta E_e}{dx} = \frac{\kappa}{2}x(2-3x) \tag{33}$$

From these expressions, we observe that the maximum of ΔE_e is located at $x = 2/3$, whereas the maximum of $\frac{d\Delta E_e}{dx}$ is found at

$x = 1/3$. Through these values, we can analyze the different stages of the process. At $x = 1/3$, the system loses its capacity to store energy and the process enters a metastable regime. At $x = x_c$, the capacity to respond effectively to the action of the external load decreases and the process enters an unstable state. Finally, at $x = 2/3$, the system cannot store more energy in the form of elastic energy and falls into an imminent failure regime.

On the other hand, the energy dissipated (**Eq. 15**) is

$$\Delta E_d \approx \frac{x}{f}\left(1 - \frac{x}{2}\right) + x - \frac{\kappa}{12}(4 - 3x)x^3, \tag{34}$$

which decreases when κ increases because at a large elastic constant, more elastic energy can be stored to be subsequently transformed into kinetic energy after the breaking of the fibers. The first derivative of the energy dissipated, given by

$$\frac{d\Delta E_d}{dx} \approx \frac{1}{f}(1 - x) + 1 - \kappa(1 - x)x^2, \tag{35}$$

must be positive, according to the second law which imposes that $0 \le \kappa \le 13/2$, for $f \gg 1$. Combining this restriction with that inherent to **Eq. 29**, we conclude that the stretching process is feasible for $0 \le \kappa \le 4$. Analyzing the derivative of the dissipated energy, we find that it has a minimum at $x \approx 2/3$, located close to the maximum of the elastic energy. The dissipated energy may thus give us information about the transition to the imminent failure regime.

Finally, the reversible heat Q_r is obtained by using **Eq. 7**:

$$Q_r = W - \Delta E_d - \Delta E_e - \Delta E_b \tag{36}$$

Its derivative with respect to the elongation

$$\frac{dQ_r}{dx} = -\ln x - \frac{1}{f}(1 - x) - 1 - \kappa x(1 - x)^2 \tag{37}$$

shows that the maximum of Q_r depends on κ and is given by

$$x^* \approx \left(368 - 54\kappa + 4\kappa^2\right)/1000. \tag{38}$$

From this expression, one can see that for $\kappa \ge 3/4$, the maximum of Q_r lies before the maximum of the derivative of the elastic energy. This result indicates that by measuring the maximum of the reversible heat (the point at which the process becomes exothermic $dQ_r/dx < 0$), we can know beforehand what is the state at which the system reaches the metastable regime. For $0 \le \kappa \le 3/4$, the maximum lies in between $x = 1/3$ and $x = 0.368$, that is, in the metastable region.

Another way to find alarming signals is to calculate the intersection point of the curves $d\Delta E_e/dx$ and dQ_r/dx, x^*, which can be obtained from **Eqs. 33**, **37**, for $f \gg 1$:

$$x^* \approx \left(368 - 118\kappa + 24\kappa^2 - 2\kappa^3\right)/1000. \tag{39}$$

For $1/3 \le \kappa \le 4$, this point is located at the metastable regime. Thus, by measuring the heat released and computing the elastic energy, we can estimate the value of elongation just before the system enters the metastable region. Finally, from **Eq. 28**, we see that for $1 \le \kappa \le 9/4$, the minimum of the stretching velocity is located before the maximum of the change of the elastic energy ($x = 1/3$), whereas for $9/4 \le x \le 4$ it is situated in the metastable regime, before the process reaches the unstable stage.

4.2 Fokker–Planck Approach

To analyze the dynamic and the energetics of the process in the case in which fluctuations are not necessarily small, we will use the Fokker–Planck equation (**Eq. 21**) from which we can obtain the average elongation of the fibers and the energy dissipated. We have solved this equation by implementing the finite difference method in the software MATLAB 2017b. The results for ρ, represented in **Figure 3**, show a Gaussian-like behavior. We can observe that as the process progresses, the solution displaces to the right. In the inset, we represent the variance for $f \gg 1$, which increases linearly with the elongation of the fibers. The small value of the variance indicates that the assumption of small fluctuations is justified in this case.

By using **Eqs. 2**, **22**, we compute the average elongation and the number of non-broken fibers which are represented in **Figure 4**. Both quantities exhibit a quasi-linear behavior and an asymptotic behavior close to the breaking point. This comes from the fact that by decreasing the number of non-broken fibers, the force

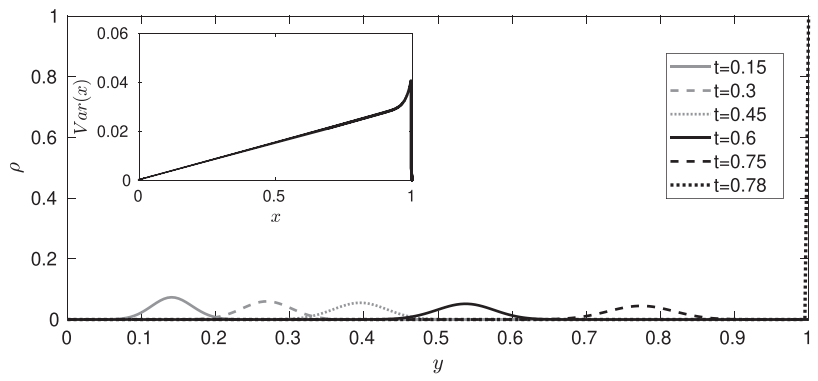

FIGURE 3 | Probability density as a function of the elongation y at different times, for $\kappa = 2$. Gaussian-like solutions displace to the right because of the action of the external force. The inset shows the variance of the probability distribution as a function of the average elongation of the set of fibers x. The variance increases linearly, then nonlinearly, and finally it decays to zero.

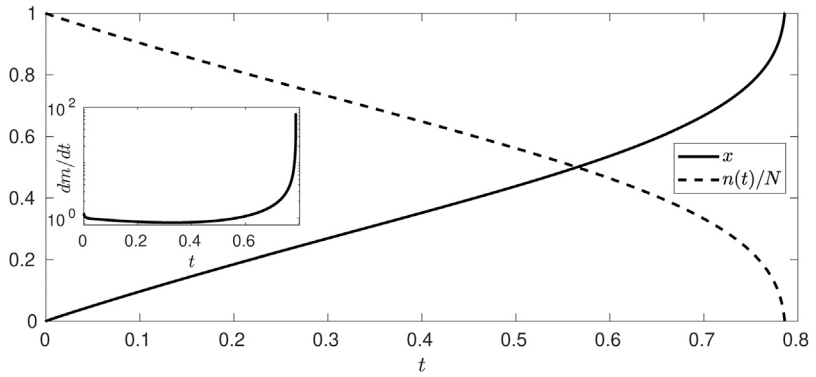

FIGURE 4 | Average elongation of the set of fibers x (continuous line) and fraction of non-broken fibers n/N (dashed line) as a function of time t, for $\kappa = 2$. The inset represents the rate of damage to the fiber bundle, which exhibits a non-monotonic behavior, thus evidencing the competition between elastic and external forces in the stretching process.

exerted per fiber increases, thus triggering an accumulative effect, typical of catastrophic events. The inset of the figure shows a non-monotonic behavior of the damage rate, evidencing the competition between the elastic and external forces in the stretching process in which finally the load force per fiber becomes much higher and the rate increases exponentially.

The stretching velocity $\dot{x}$ follows from the dynamics of x. By taking the derivative of $\dot{x}$ with respect to x, we obtain the change of the stretching velocity as a function of the average elongation. In **Figure 5**, we show the behavior of both quantities for $\kappa = 2$. We observe the existence of a minimum of the stretching velocity around $x = 0.29$ which appears before the system reaches the maximum change of the elastic energy (the transition toward the metastable regime).

From the dynamics of the process, we can calculate the energy dissipated by using **Eqs. 14**, **15**, **17**. **Figure 6** shows the energetics of the process. As predicted from the analytical results, we observe a maximum of the elastic energy and of the reversible heat. Furthermore, the maximum of Q_r is located around $x = 0.366$, independently of the values of κ. Additionally, the net reversible heat at the end of the process ($Q_r(x = 1)$) is zero, which shows that the stretching process is endothermic at small deformations and exothermic at larger deformations. The irreversible heat released results in measurable changes in the temperature of the environment.

The derivatives of the different energies with respect to x are represented in **Figure 7**. Before the imminent failure regime, the behavior of the temporal derivatives coincides with that of the spatial derivatives due to the fact that in this regime, x is linear in time, as follows from **Eq. 29**. The results obtained confirm that the derivative of the elastic energy has a maximum at $x = 1/3$ and its primitive a maximum at $x = 2/3$, while the derivative of the breaking energy always grows. They also confirm that both derivatives take the same value at $x = 1/2$. The derivative of the reversible heat always decreases, which indicates that the net flux of reversible heat is much higher at the beginning of the process. The curve of this derivative intersects that of the derivative of the elastic energy around $x = 1/5$, for $\kappa = 2$, while for lower values of κ, the intersection point moves to the right, being $\kappa = 1/2$ the highest value of κ at which the crossing takes place before the process reaches the metastable regime.

From **Figure 7**, we also confirm the fact that the derivative of the dissipated energy is always positive, in accordance with the second law of thermodynamics. Interestingly, the minimum of this derivative is found around $x = 1/2$ (independently of the

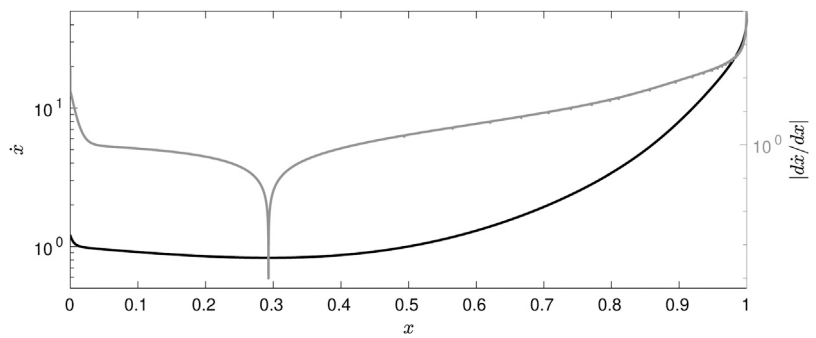

FIGURE 5 | Stretching velocity $\dot{x}$ (left grid, black continuous line) and absolute value of $d\dot{x}/dx$ (right grid, gray continuous line) as a function of the average elongation x, for $\kappa = 2$ represented in the logarithmic scale.

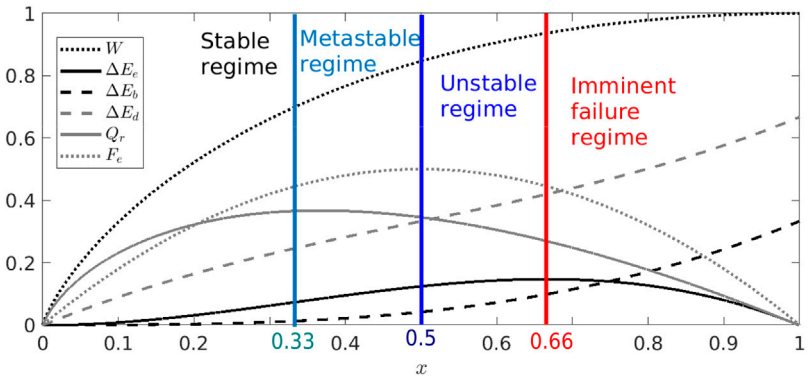

FIGURE 6 | Energetics as the stretching progress, for $\kappa = 2$. The work done W (dotted black line) is computed from **Eq.10**, the elastic energy ΔE_e (continuous black line) is computed from **Eq. 8**, the breaking energy ΔE_b (dashed black line) is computed from **Eq. 9**, the dissipated energy ΔE_d (dashed gray line) is computed from **Eqs. 14**, **17**, and the reversible heat Q_r (continuous gray line) is computed from **Eqs. 7**, **12**. The metastable regime threshold (light blue line) is located at $x = 1/3$, the unstable regime threshold (blue line) is located at $x = 1/2$, while the imminent failure threshold (red line) is located at $x = 2/3$.

value of κ), which is the same value at which the derivatives of the elastic and breaking energy coincide.

4.3 Role of the Fluctuations in the Stretching Process

The role that fluctuations play in the process can be estimated by comparing the value of the relevant quantities when we use the small fluctuation approach or when we adopt a Fokker–Planck description for the same value of κ. **Figure 8** shows the change of the stretching velocity with position. In particular, for $\kappa = 2$, the location of the minimum of this quantity computed from both approaches is the same, meaning that close to the minimum the system is practically insensitive to the presence of fluctuations. However, for small elongations, the velocities are slightly different, while at the imminent failure regime, they differ considerably due to the presence of fluctuations.

As shown in **Figure 9**, energy dissipation and reversible heat are affected by fluctuations at all stages of the process. The dissipated energy is overestimated in the approach of small fluctuations, whereas the reversible net heat $(Q_r(x = 1))$ is very sensitive to fluctuations, as concluded from the fact that this quantity is different in both approaches.

Figures 8, **9** show that the small fluctuation approach adequately describes the dynamics but not the energetics. The high accuracy in the dynamics is due to the almost Gaussian nature of the probability with a sufficiently small variance which is represented in **Figure 3**. The observed disparity in the reversible heat and energy dissipated lies in the approximation used. Additionally, the small deviation of the stretching velocity is accumulated, thus affecting the energy dissipated in the case of small fluctuation. Differences between both approaches become even more patent at smaller values of κ and f when the effect of the fluctuations is less important.

5 CONCLUSION

We have proposed a thermodynamic framework that analyses the role played by dissipation in a fiber stretching process, describes

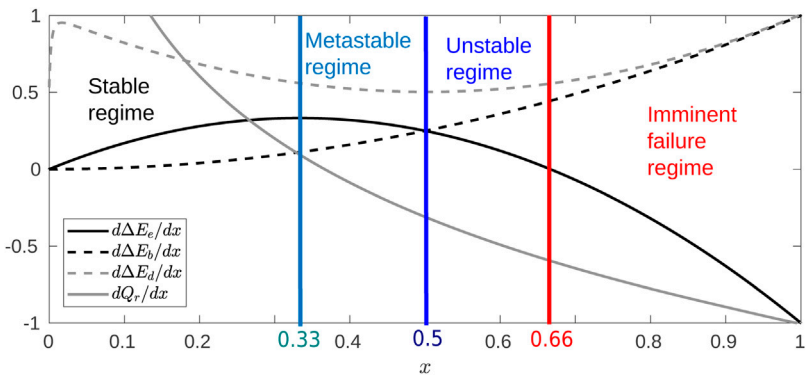

FIGURE 7 | Derivatives for the energies of the stretching process as a function of the average elongation x, for $\kappa = 2$. $d\Delta E_e/dx$: continuous black line; $d\Delta E_b/dx$: dashed black lines; $d\Delta E_d/dx$: dashed gray line; and dQ_r/dx: continuous gray line. Metastable regime transition: light blue line at $x = 1/3$; unstable regime transition: blue line at $x = 1/2$; and imminent failure regime transition: red line at $x = 2/3$.

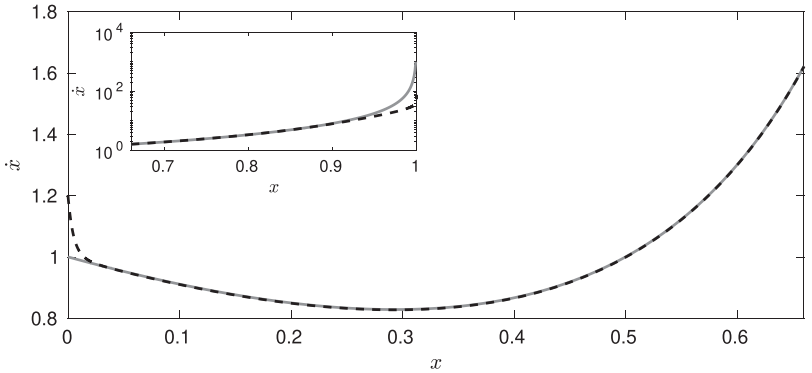

FIGURE 8 | Results for the stretching velocity $\dot{x}$ as a function of the average elongation x before the imminent failure regime, for $\kappa = 2$. The inset shows $\dot{x}$ in the imminent failure regime. The continuous gray line is obtained by assuming small fluctuations, while the dashed black line shows the behavior of that quantity for larger fluctuations obtained from the numerical solution of the Fokker–Planck equation.

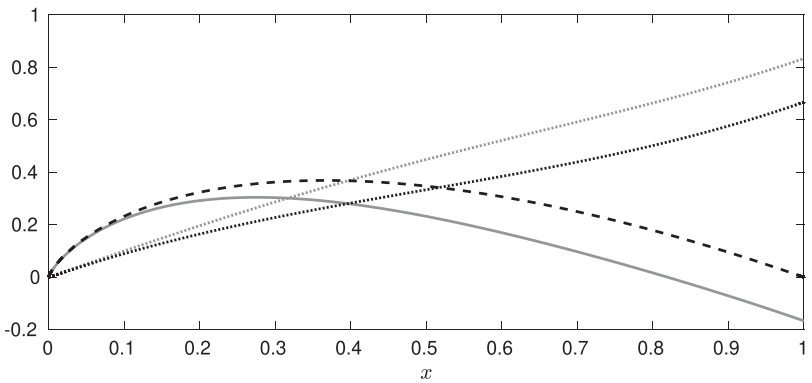

FIGURE 9 | Dissipated energy and reversible heat as a function of the average elongation x, for $\kappa = 2$. Results for ΔE_d and Q_r obtained when fluctuations are small are represented, respectively, by dotted and continuous gray lines. The same quantities for larger fluctuations, computed from the Fokker–Planck equation, correspond to the dotted and dashed black lines, respectively.

its different stages, and obtains new alarming signals before the whole set of fibers break. Our thermodynamic framework has identified relevant regimes (metastable, unstable, and imminent failure) as well as provided new transition indicators in terms of stretching velocity variation and entropy production rate, which is an important quantity to measure the energy efficiency of processes [27]. Specifically, we have shown that the maximum of the reversible heat may emerge before the process enters into the unstable regime. For some values of κ and small fluctuations, this maximum is located in the stable regime. In the same line, we found that the minimum of the entropy production rate is located around the transition to the unstable regime, and that for small fluctuations, this minimum defines the starting of the imminent failure regime for all values of κ. We have also proved that when the heat release flux is equal to the entropy production rate, in this intersection, the system is close to the transition toward the metastable regime. Similarly, we found that the minimum of the stretching velocity is always located in the stable zone, but the exact location strongly depends on the value of κ.

Under this approach, a more general analysis of the stretching process as a function of $\kappa = k_e L_m/F$ could be performed to investigate the effect of the relation between force and elastic constant on the dynamics. Additionally, for a small system with a low number of fibers, the approach can be applied to investigate biological stretching failure processes such as fiber muscle elongations and biochemical stretching as in DNA chains. Finally, as the stretching process releases heat and dissipates energy, we can have considerable temperature changes which can influence the individual failure of elements [28–30]. Further work is therefore needed on this issue.

DATA AVAILABILITY STATEMENT

The raw data supporting the conclusions of this article will be made available by the authors, without undue reservation.

AUTHOR CONTRIBUTIONS

AAR and JMR developed the idea, proposed the thermodynamic formalism used, and wrote the first version of

the article. SP suggested the problem and supervised the results obtained. All authors contributed equally to the discussion of the manuscript.

ACKNOWLEDGMENTS

The authors are grateful to the Research Council of Norway for its Center of Excellence Funding Scheme, project no. 262644, and to PoreLab which partially funded the stay of JMR in Tronndheim. AAR and JMR acknowledge financial support of MICIU (Spanish government) under Grant No. PGC2018–098373-B-I00 and of the Catalan government under Grant 2017-SGR-884. AAR is grateful for the financial support through an APIF 2017–2018 scholarship from the University of Barcelona. We would like to thank Signe Kjelstrup, Dick Bedeaux, Alex Hansen, and in general the members of PoreLab for interesting discussions during the visit of two of us (JMR and AAR) to PoreLab.

REFERENCES

1. Chakrabarti BK, and Benguigui LG. *Statistical Physics of Fracture and Breakdown in Disordered Systems*. 55 Oxford and New York, NY: Oxford University Press (1997). 176 p.
2. Herrmann HJ, and Roux S. *Statistical Models for the Fracture of Disordered Media*. North Holland: Elsevier (1990). 353 p.
3. Biswas S, Ray P, and Chakrabarti BK. *Statistical Physics of Fracture, Breakdown, and Earthquake: Effects of Disorder and Heterogeneity*. Weinheim, Germany: John Wiley & Sons (2015). 344 p.
4. Peirce FT. Tensile Tests for Cotton Yarns: "The Weakest Link" Theorems on the Strength of Long and of Composite Specimens. *J Textile Inst* (1926) 17: T355–368. doi:10.1080/19447027.1926.10599953
5. Pradhan S, Hansen A, and Chakrabarti BK. Failure Processes in Elastic Fiber Bundles. *Rev Mod Phys* (2010) 82:499–555. doi:10.1103/RevModPhys.82.499
6. Hansen A, Hemmer PC, and Pradhan S. *The Fiber Bundle Model: Modeling Failure in Materials*. Weinheim, Germany: John Wiley & Sons (2015). 256 p.
7. Pradhan S, and Chakrabarti BK. Precursors of Catastrophe in the Bak-Tang-Wiesenfeld, Manna, and Random-Fiber-Bundle Models of Failure. *Phys Rev E* (2001) 65:016113. doi:10.1103/PhysRevE.65.016113
8. Hemmer PC, and Hansen A. The Distribution of Simultaneous Fiber Failures in Fiber Bundles. *J Appl Mech* (1992) 59:909–14. doi:10.1115/1.2894060
9. Pradhan S, Hansen A, and Hemmer PC. Crossover Behavior in Burst Avalanches: Signature of Imminent Failure. *Phys Rev Lett* (2005) 95: 125501. doi:10.1103/PhysRevLett.95.125501
10. Pradhan S, and Hemmer PC. Relaxation Dynamics in Strained Fiber Bundles. *Phys Rev E* (2007) 75:056112. doi:10.1103/PhysRevE.75.056112
11. Reiweger I, Schweizer J, Dual J, and Herrmann HJ. Modelling Snow Failure With a Fibre Bundle Model. *J Glaciol* (2009) 55:997–1002. doi:10.3189/002214309790794869
12. Cohen D, Lehmann P, and Or D. Fiber Bundle Model for Multiscale Modeling of Hydromechanical Triggering of Shallow Landslides. *Water Resour Res* (2009) 45:W10436. doi:10.1029/2009WR007889
13. Pollen N, and Simon A. Estimating the Mechanical Effects of Riparian Vegetation on Stream Bank Stability Using a Fiber Bundle Model. *Water Resour Res* (2005) 41:W07025. doi:10.1029/2004WR003801
14. Pugno NM, Bosia F, and Abdalrahman T. Hierarchical Fiber Bundle Model to Investigate the Complex Architectures of Biological Materials. *Phys Rev E* (2012) 85:011903. doi:10.1103/PhysRevE.85.011903
15. Sornette D. Mean-Field Solution of a Block-Spring Model of Earthquakes. *J Phys France* (1992) 2:2089–96. doi:10.1051/jp1:1992269
16. Daniels HE, and Jeffreys H. The Statistical Theory of the Strength of Bundles of Threads. I. *Proc R Soc Lond Ser A. Math Phys Sci* (1945) 183:405–35. doi:10.1098/rspa.1945.0011
17. Sornette D. Elasticity and Failure of a Set of Elements Loaded in Parallel. *J Phys A: Math Gen* (1989) 22:L243–50. doi:10.1088/0305-4470/22/6/010
18. Harlow DG, and Phoenix SL. Approximations for the Strength Distribution and Size Effect in an Idealized Lattice Model of Material Breakdown. *J Mech Phys Sol* (1991) 39:173–200. doi:10.1016/0022-5096(91)90002-6
19. Hidalgo RC, Moreno Y, Kun F, and Herrmann HJ. Fracture Model With Variable Range of Interaction. *Phys Rev E* (2002) 65:046148. doi:10.1103/PhysRevE.65.046148
20. Pradhan S, Kjellstadli JT, and Hansen A. Variation of Elastic Energy Shows Reliable Signal of Upcoming Catastrophic Failure. *Front Phys* (2019) 7:106. doi:10.3389/fphy.2019.00106
21. Bering E, Kjelstrup S, Bedeaux D, Rubi JM, and de Wijn AS. Entropy Production Beyond the Thermodynamic Limit From Single-Molecule Stretching Simulations. *J Phys Chem B* (2020) 124:8909–17. doi:10.1021/acs.jpcb.0c05963
22. Li D, Ou J, Lan C, and Li H. Monitoring and Failure Analysis of Corroded Bridge Cables Under Fatigue Loading Using Acoustic Emission Sensors. *Sensors* (2012) 12:3901–15. doi:10.3390/s120403901
23. De Groot SR, and Mazur P. *Non-Equilibrium Thermodynamics*. New York, NY: Courier Corporation (2013). 510 p.
24. Bejan A, Tsatsaronis G, and Moran M. *Thermal Design and Optimization*. New York, NY: John Wiley & Sons (1996). 560 p.
25. Rubi JM, Bedeaux D, and Kjelstrup S. Thermodynamics for Single-Molecule Stretching Experiments. *J Phys Chem B* (2006) 110:12733–7. doi:10.1021/jp061840o
26. Reguera D, Rubí JM, and Vilar JMG. The Mesoscopic Dynamics of Thermodynamic Systems. *J Phys Chem B* (2005) 109:21502–15. doi:10.1021/jp052904i
27. Kjelstrup S, Bedeaux D, Johannessen E, and Gross J. *Non-Equilibrium Thermodynamics for Engineers*. 2nd ed. World Scientific (2017). 510 p.
28. Roux S. Thermally Activated Breakdown in the Fiber-Bundle Model. *Phys Rev E* (2000) 62:6164–9. doi:10.1103/PhysRevE.62.6164
29. Pradhan S, and Chakrabarti BK. Failure Due to Fatigue in Fiber Bundles and Solids. *Phys Rev E* (2003) 67:046124. doi:10.1103/PhysRevE.67.046124
30. Pradhan S, Chandra AK, and Chakrabarti BK. Noise-Induced Rupture Process: Phase Boundary and Scaling of Waiting Time Distribution. *Phys Rev E* (2013) 88:012123. doi:10.1103/PhysRevE.88.012123

Conflict of Interest: The authors declare that the research was conducted in the absence of any commercial or financial relationships that could be construed as a potential conflict of interest.